NAL TR-640T

UDC 621. 45. 034. 36
532. 517

TECHNICAL REPORT OF NATIONAL AEROSPACE LABORATORY

TR-640T

A Theoretical Analysis of Laminar and Turbulent Swirling Flows in Cylindrical Annuli*

Atsumasa YAMAMOTO and D.A.J MILLAR

November 1980

NATIONAL AEROSPACE LABORATORY

CHŌFU, TOKYO, JAPAN

A Theoretical Analysis of Laminar and Turbulent Swirling Flows in Cylindrical Annuli

Atsumasa YAMAMOTO** and D.A.J. MILLAR***

ABSTRACT

An implicit numerical method and the results of laminar and trubulent swirling flows in cylindrical annuli are presented. The study was motivated by the need to analize the decay of a swirl component of velocity along an annular duct, one of the important features in turbomachinery, and one which could not be predicted by methods based on an inviscid flow assumption. A set of parabolized Navier-Stokes equations is used for the basic equations governing the flow. In the case of turbulent flow, they are solved in conjunction with two additional transport equations which give the necessary turbulent eddy viscosity for use in the basic flow equations. The numerical solutions are compared to some laminar solutions and to some turbulent experimental data. On the basis of the calculated results, the present approach showed many possible patterns and characteristics of the flow.

概　　要

二重円環内における層流及び乱流旋回流に関する数値計算の方法と結果について述べた。本報告はタービ機械等でみられる旋回流れの円周方向速度成分の下流での減衰の予測を主な目的としたものであり，この予測はタービ機械の設計や性能予測でよく用いられる非粘性の仮定を基礎とした計算方法では不可能なものである。計算の方法としては放物化したナビアトークス方程式に乱流モデルとしての乱流エネルギーとその散逸率に関する二輸送方程式を組合せて解く。計算結果は層流，乱流および旋回速度の有無の組合せの各場合について，他の解析解，数値解，現在入手出来る実験結果等と比較し，本方法の有効性，問題点，改良点について議論した。

NOMENCLATURE

English Symbols

a, b, c, d	= coefficients used in Eq. 4 (see Table 2)
A, B, C, D, F L, S, T, V	= coefficients used Eqs. 9-10, or constants used in Eq. 6
C_1, C_2, C_μ	= empirical constants used in Eqs. 3 and in Table 2
D_h	= hydraulic diameter, $D_h = 2(r_o - r_i)$
E	= constant used in Eq. 5
K	= von Karman constant used in Eq. 5
P	= static pressure
r	= radius
Re	= Reynolds number based on mean axial velocity, molecular viscosity and D_h
Re_{mesh}	= Reynolds number based on mean axial velocity, effective viscosity and mesh $(\Delta r)^2/\Delta z$
U_{av}, U_{max}, U	= average, maximum and local velocities
W	= time averaged velocity
y	= distance normal to wall measured from wall
z	= axial distance measured from inlet (or initial) station
$\Delta r, \Delta z$	= small space in radial, and axial directions in Fig. 1

* Received 3, September 1980

** Aeroengine Division

*** Carleton University, Mechanical & Aeronautical Engineering, Ottawa, Canada

Greek Symbols

ϵ	= rate of dissipation of turbulent kinetic energy
κ	= turbulent kinetic energy
μ, μ_t	= molecular and turbulent viscosities
μ_{eff}	= effective viscosity, $\mu_{eff} = \mu + \mu_t$
ν	= kinematic viscosity, $\nu = \mu/\rho$
ρ	= fluid density
η	= non-dimensional distance used in Eq. 6
ψ	= variable representing one of rW_θ, $\omega/r, \Psi, \kappa$ and ϵ
ϕ	= swirl angle defined by $\tan^{-1}(W_\theta/W_z)$
Ψ	= stream function defined by Eq. 1
$\sigma_\kappa, \sigma_\epsilon$	= empirical constants in Table 2
$\Sigma_{AB}, \Sigma_{ABS}$	= coefficients used in Eq. 10
ω	= vorticity defined by Eq. 2

Subscripts

B	= denotes value at a location B normal to wall (i.e., $y_B = 30\nu/W^*$ or $y^+ = 30$)
eff	= effective
n', p', s'	
$N, P (=p), S, NU, PU (=pu), SU$	= denote locations shown in Fig. 2 where values are evaluated
r	= radial
z	= axial
θ	= tangential
ψ	= denotes value corresponding to variable ψ

Superscripts

+	= non-dimensional distance of y, $y^+ = W^* y/\nu$
–	= mean
*	= friction velocity

INTRODUCTION

Swirling flow is an important and basic feature of turbomachinery. For example, the flow at the exit of an axial compressor blade row has a strong swirl, or circumferential, component of velocity. This swirl velocity will decay along the duct due mainly to the viscous force between fluid and the duct walls and between the fluid particles themselves. Depending on the axial spacing between this rotor and the subsequent stator, the change in flow angle due to the decay of swirl velocity may cause the incidence angle of the stator to be mismatched and may drop the performance of this blade row, if this decay is not considered in the design of the stator blade row. This situation could be serious in current turbomachinery designs; for example, in the fan stage of a turbofan engine, a fairly large axial space between rotor and stator is required to reduce the fan noise generated by blade wake/stator interaction. The same problem can arise in an inter-turbine duct which has a large distance between the high pressure and low pressure turbine stages.

On the other hand, the most widely used and comprehensive methods for predicting the internal flow of turbomachinery are the streamline curvature and matrix methods e.g., Davis et al. [1], and both of these methods assume essentially inviscid flow between blade rows. As tools for predicting the performance of a machine and for the design, both methods have worked adequately for conventional machines, although the results depend strongly on the empirical cascade performance data used with the basic inviscid flow equations. Since the methods are basically inviscid, annulus boundary layer is usually calculated to get more realistic flow picture. However, this modification does not affect the swirl component significantly, since the main purpose is a calculation of blockage of annular area. Moreover, in the calculation methods of skewed flows, no satisfactory means for patching the inviscid flow region to the viscous flow or boundary layer region and for taking account of the interaction effect of two different shear layers has been developed. The present study was initiated to overcome the deficiency of the inviscid methods in calculating a turbulent swirling flow field, because of the practical importance of the problem in turbomachinery design and analysis.

In the present paper, a numerical calculation method for both laminar and turbulent swirling flows in stationary annuli without patching the flows is briefly described and the performance by the method is presented. The method employs the so-called "parabolized" Navier-Stokes equations to

Table 1 Some Calculation Methods for Swirling Flows in Pipes and Annular Ducts

Authors, Year	Type of Flows	Type of Solutions	Type of Ducts	Viscosity used	Other Features
Gollatz et. al., 1954	Laminar	Analytical	Pipe	Constant	Eigen Value Problem
Talbot, 1954	Laminar	Analytical	Pipe	Constant	Stabilizing Effects
Dissler et. al., 1960	Turbulent	Analytical	Pipe	Constant	
Kreith et. al., 1965	Turbulent	Analytical	Pipe	Algebraically distributed	Decay of Tape induced Swirl
Rochino et. al., 1968	Turbulent	Analytical	Pipe		
Scott, 1972	Turbulent	Analytical	Annulus	Constant	Series solution
Scott et. al., 1976	Turbulent	Analytical	Annulus	Algebraically distributed	
Boerner, 1970	Turbulent	Numerical	Annulus	Algebraically distributed	Elliptic Form of N. S. Eq's.
Sharma et. al., 1976	Turbulent	Numerical	Annulus	Mixing length hypothesis	Parabolic Form of N. S. Eq's.

describe the basic flow and another two transport equations to describe turbulence phenomena statistically; a differential type of turbulence model using the turbulent kinetic energy and the dissipation (so-called κ-ϵ model) by Launder and Spalding has been chosen, which has been used in several examples [2, 3] for non-swirling flows. For the swirling flow problem in stationary annuli, however, experience with this model appears to be scarce. In the present study, the equilibrium or universal law of the wall is applied in order to describe the axial and tangential velocities near both of the inner and outer walls. Table 1 shows the summary of review on the calculation methods of swirling flow in pipes and annuli.

MATHEMATICAL FORMULATION

The Basic Governing Equations and The Turbulence Model. The next three major assumptions are made on the equations of motion and continuity: (1) The flow is assumed to be incompressible, axisymmetrical and steady, without body forces. (2) The axial viscous diffusion terms, i.e., the second order derivatives in the axial direction in the viscous terms are omitted from all momentum equations. (3) In turbulent flow case, the "eddy viscosity concept" is introduced. The definitions of stream function Ψ and vorticity ω used in the present study are

$$\frac{\partial \Psi}{\partial r} = \rho r W_z, \quad \frac{\partial \Psi}{\partial z} = -\rho r W_r \tag{1}$$

$$\omega = \frac{\partial W_r}{\partial z} - \frac{\partial W_z}{\partial r} \tag{2}$$

These two functions Ψ and ω are introduced into the basic governing equations to eliminate the equation of continuity and the two pressure terms from the governing equations.

In the case of turbulent flows, a two-equation (κ-ϵ) model of turbulence is employed, which provides the turbulent eddy viscosity as follows [3]:

$$\mu_t = C_\mu \rho \kappa^2/\epsilon \tag{3}$$

To calculate μ_t from turbulent kinetic energy κ and the dissipation rate ϵ, two transport equations for κ and ϵ have to be solved.

The final forms of the basic governing equations and the transport equations can be expressed in the following compact form where a notation of ψ is used as a general term representing one of the five variables: angular momentum rW_θ, vorticity function ω/r, the stream function Ψ, κ and ϵ:

$$a_\psi \frac{\partial}{\partial z}(r \rho W_z \cdot \psi) = -a_\psi \frac{\partial}{\partial r}(r\rho W_r \cdot \psi) + \frac{\partial}{\partial r}\left\{ b_\psi r \frac{\partial (c_\psi \cdot \psi)}{\partial r} \right\} - r d_\psi \tag{4}$$

where a_ψ, b_ψ, c_ψ and d_ψ are coefficients of the above partial differential equations, corresponding to each variable ψ and are tabulated in Table 2, where σ_κ, σ_ϵ, C_1 and C_2 are empirical constants, the recommended values of which are $C_\mu = 0.09$, $C_1 = 1.44$, $C_2 = 1.92$, $\sigma_\kappa = 1.0$ and $\sigma_\epsilon = 1.3$. It may be doubtful whether these empirical constants would work well in problems such as the present study, for which experimental data is scarce and was not used to define the constants. In the absence of more reliable values based on relevant experimental information, however, this study will employ the above suggested values for the constants.

The Boundary Conditions. Fig. 1 shows schematically the boundary conditions used. To calculate turbulent flows economically, the equilibrium law of the wall is adopted:

Table 2 Coefficients in Equation (4)

ψ	a_ψ	b_ψ	c_ψ	d_ψ
rW_θ	1	$\mu_{off,\theta} r^2$	$1/r^2$	0
$\frac{\omega}{r}$	r^2	r^2	$\mu_{off,z}$	$-\frac{\partial}{\partial z}(\rho W_\theta^2)$
Ψ	0	$1/\rho r^2$	1	$-\omega/r$
κ	1	$\frac{\mu_t}{\sigma_\kappa}+\mu$	1	$\rho\epsilon - \{\mu_{t,z}(\frac{\partial W_z}{\partial r})^2 + \mu_{t,\theta}(\frac{\partial W_\theta}{\partial r}-\frac{W_\theta}{r})^2\}$
ϵ	1	$\frac{\mu_t}{\sigma_\epsilon}+\mu$	1	$\frac{\epsilon}{\kappa}[C_2\rho\epsilon - C_1\{\mu_{t,z}(\frac{\partial W_z}{\partial r})^2 + \mu_{t,\theta}(\frac{\partial W_\theta}{\partial r}-\frac{W_\theta}{r})^2\}]$

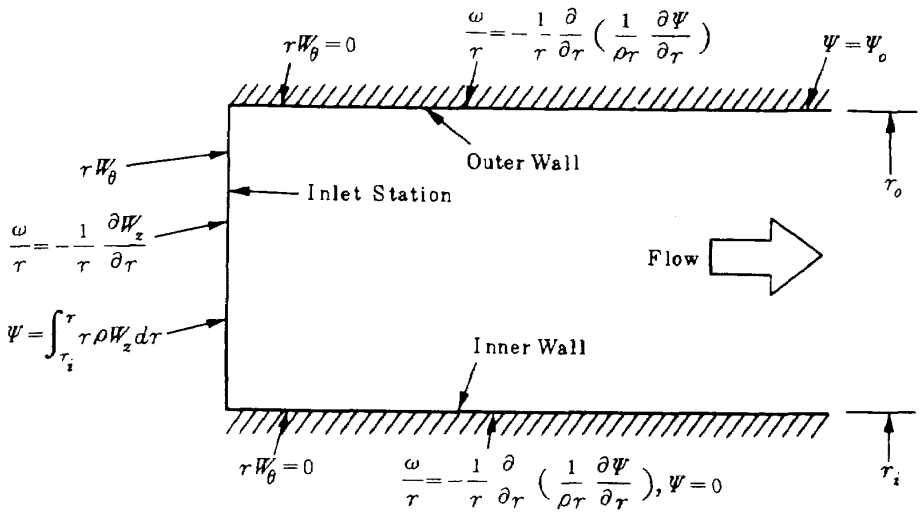

(a) B.C. for rW_θ, ω/r and Ψ (See N.B.)

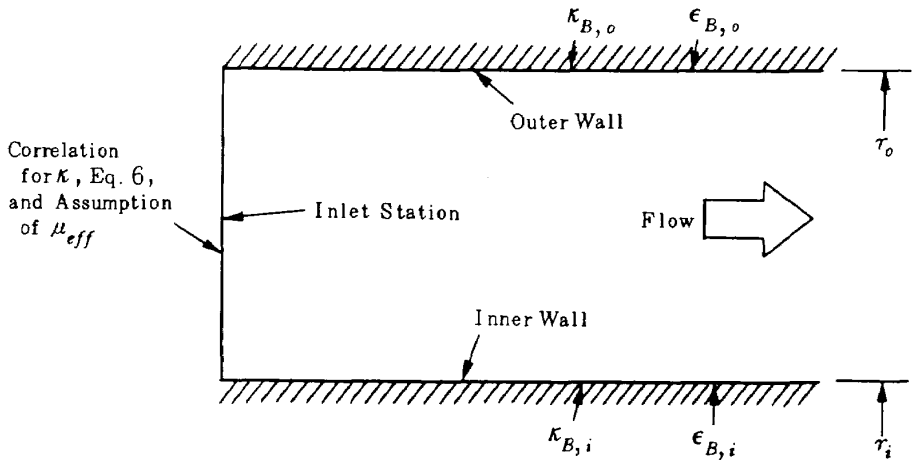

(b) B.C. for κ and ϵ

Fig. 1 Schematic Drawing of Boundary Conditions

N. B. / In turbulent flow case, the modification by the law of the wall, Eq. 5, is used.

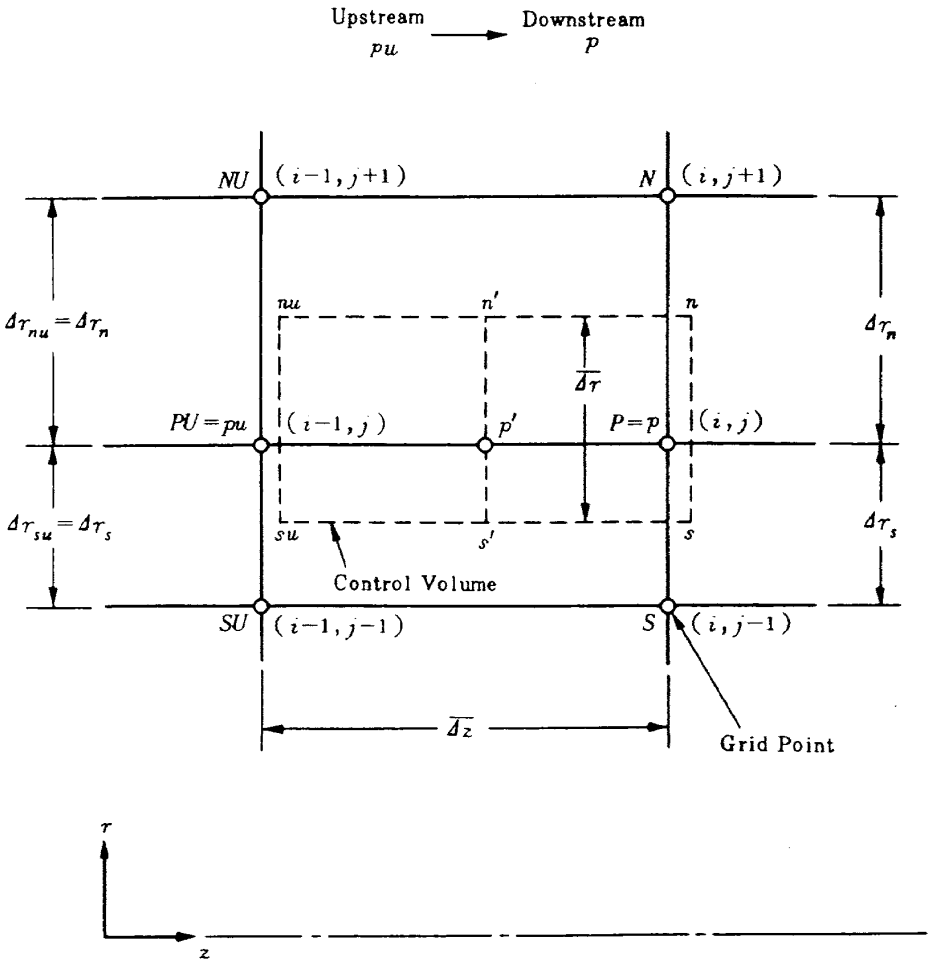

Fig. 2 Finite Difference Scheme for Cylindrical Coordinates

$$W = \frac{W^*}{K} \ell n \frac{EW^*}{\nu} y \qquad (5)$$

where W^* is the friction velocity $\sqrt{\tau_w/\rho}$, K and E are constant ($K=0.42$ and $E=9$). This distribution is assumed for both axial and tangential velocities (i.e., $W \equiv W_z$ or W_θ) near the walls up to the distance of $y^+ = 30$ ($=\nu y/W^*$) from the wall. For κ, an experimental correlation between κ and velocity field proposed by Bobkov et al. [4] is used to determine the inlet κ from the inlet velocities which are usually known. The formula used here is

$$\kappa = A e^{-B\eta} U^2 (1 - \frac{U_{av}}{U_{max}})^2 \qquad (6)$$

where A and B are constant ($A=0.7225$ and $B=2.54$ are used here), η is non-dimensional and is the distance normal to the wall divided by the distance from the wall to the point of maximum velocity. U, U_{av} and U_{max} are local, average and maximum velocity respectively. Although Bobkov's correlation was found from flows without swirl in various types of duct geometries including annuli, it is assumed in the present calculation that the total velocity $(W_z^2 + W_r^2 + W_\theta^2)^{1/2}$ is used instead of U. Effective viscoisty is sometimes known experimentally and the initial viscoisty is, therefore, often given to start the calculation instead of the inlet ϵ value. The wall boundary conditions for κ and ϵ are determined by:

$$\mu_{t,z} (\frac{\partial W_z}{\partial r})^2 + \mu_{t,\theta} (\frac{\partial W_\theta}{\partial r} - \frac{W_\theta}{r})^2 = \rho\epsilon \qquad (7)$$

which was reduced from κ equation, assuming that convection and diffusion of κ are negligible near the walls. Also assuming that $\mu_{t,z} = C_{\mu,z}\rho\kappa^{1/2}\ell$ and $\mu_{t,\theta} = C_{\mu,\theta}\rho\kappa^{1/2}\ell$ by analogy to Eq. 3 and ℓ is proportional to the distance y, near the wall, one may express the values of κ_B and ϵ_B near the walls (at $y = y_B$). These values, κ_B and ϵ_B, were used as the values on the wall since this could improve the convergence of solution

without serious computational error rather than applying the κ_B and ϵ_B exactly at the point $y=y_B$. Further details may be found in Ref. [5]

Numerical Scheme and The Stability Condition. The Crank-Nicolson implicit scheme can avoid the serious divergence problem coming from the numerical scheme and does not increase the error on passing from one station to the next. In fact, the present method was not suffered from a serious limitation for axial step size such as Patanker and Spalding's method has in non-swirling flow [6] and also did not have such difficulties of obtaining stable numerical solutions for the present case of internal swirling flow as Sharma et al. [7] describe.

The Crank-Nicolson scheme for Eq. 4, in cylindrical coordinates may be expressed by:

$$(a_\psi)_{p'} \frac{(r\rho W_z \cdot \psi)_{pu} - (r\rho W_z \cdot \psi)_p}{\Delta z} =$$

$$- (a_\psi)_{p'} \frac{\partial}{\partial r} (r\rho W_r \cdot \psi)_{p'} + \frac{\partial}{\partial r} (b_\psi r \frac{\partial (c_\psi \cdot \psi)}{\partial r})_{p'}$$

$$- (r d_\psi)_{p'} \qquad (8)$$

where subscripts pu, p and p' denote evaluating the variables and the coefficients at the upstream, downstream and mid station between pu and p, respectively (Fig. 2). Corresponding finite difference equations are

$$\psi_P = C_N \psi_N + C_S \psi_S + D \qquad (9)$$

where

$$C_N = (A_N + B_N c_{\psi,N})/\Sigma AB$$

$$C_S = (A_S + B_S c_{\psi,S})/\Sigma AB$$

$$D = (S + S_{\psi,U})/\Sigma AB$$

$$A_N = \| -\tfrac{1}{4} a_{\psi,p'} \overline{\Delta z} (r\rho W_r)_{n'} \|$$

$$A_S = \| \tfrac{1}{4} a_{\psi,p'} \overline{\Delta z} (r\rho W_r)_{s'} \|$$

$$B_N = \tfrac{1}{2} \frac{(b_\psi r)_{n'} \overline{\Delta z}}{\Delta r_n}$$

$$B_S = \tfrac{1}{2} \frac{(b_\psi r)_{s'} \overline{\Delta z}}{\Delta r_s}$$

$$\Sigma_{AB} = F_U + A_N + A_S + c_{\psi,p} (B_N + B_S) \qquad (10)$$

$$S = -d_{\psi,p'} V_{p'}$$

$$S_{\psi,U} = \{F_U - A_N - A_S - c_{\psi,PU}(B_{NU} + B_{SU})\} \psi_{PU} + C_{NU}\psi_{NU} + C_{SU}\psi_{SU}$$

$$F_U = a_{\psi,p'} (r\rho W_z)_{PU} \overline{\Delta r}$$

$$B_{NU} = B_N \frac{\Delta r_n}{\Delta r_{nu}}, \quad B_{SU} = B_S \frac{\Delta r_s}{\Delta r_{su}}$$

$$C_{NU} = A_N + c_{\psi,NU} B_{NU}, C_{SU} = A_S + c_{\psi,SU} B_{SU}$$

$$V_{p'} = r_{p'} \cdot \overline{\Delta z} \cdot \overline{\Delta r}$$

$$\| L \| = \tfrac{1}{2} (|L| + L).$$

Rose [8] expresses the stability condition for the Crank-Nicolson scheme with uniform mesh by:

$$Re_{mesh} \geq 1 \qquad (11)$$

where $Re_{mesh} = W_z (\Delta r)^2 / \Delta z \cdot \nu_{eff}$ and W_z is the mean axial velocity. In the present calculations including non-uniform mesh, to determine the mesh sizes in the radial and axial directions, $Re_{mesh} \geq 2 \sim 3$ was safely used but, for about the first ten axial steps, about one-tenth of the axial interval Δz obtained from this criterion was used for safety.

RESULTS AND DISCUSSION

All calculations presented here have been done by assuming equal axial and tangential effective viscosities.

Laminar Flow Without Swirl

Fig. 3 shows a comparison of the results by the present method and analytical solutions [9] for fully developed laminar flows in annuli of two different inner/outer radius ratios (r_i/r_o = 0.5 and 0.1). Different locations of maximum velocity may be found in the two cases. Excellent agreement of the two methods is shown. The present numerical results used 21 radial grids and about 30 axial steps up to the fully developed laminar stage, while Liu et al. [6] used a number of axial steps (>1000) to get fully developed flows by the method of Ref. [10]

Laminar Flow With Swirl

Fig. 4 shows decay of the swirl velocity downstream from an upstream solid body rotation and compares the presently calculated result with that by the Navier-Stokes equations of elliptic form [11], in which the axial viscous diffusion terms are retained.

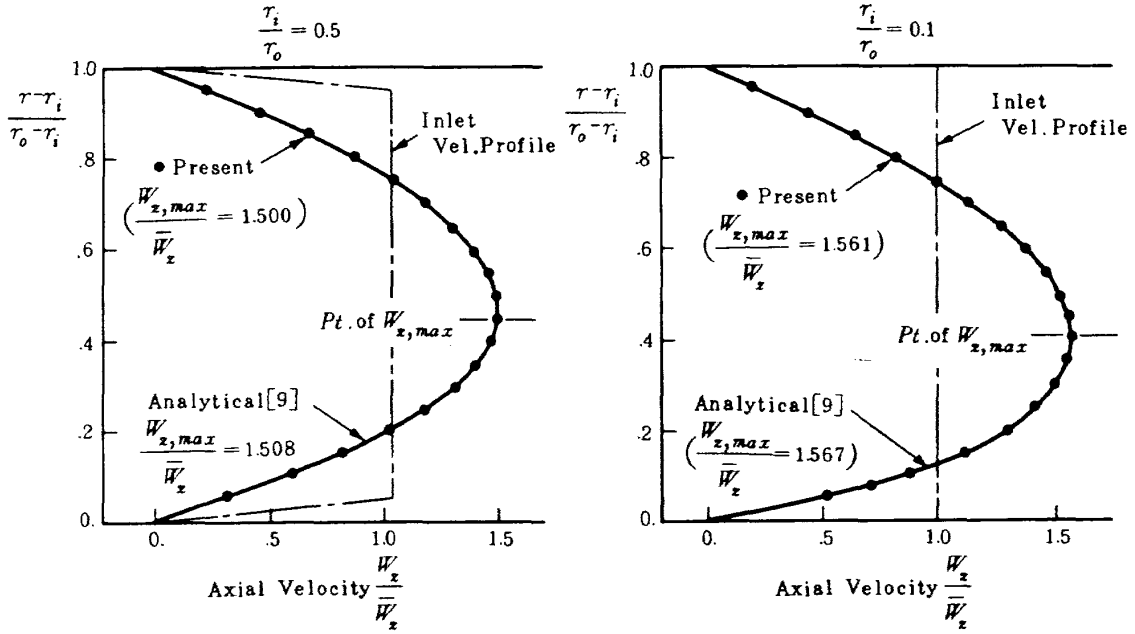

Fig. 3 Fully Developed Laminar Flow without Swirl

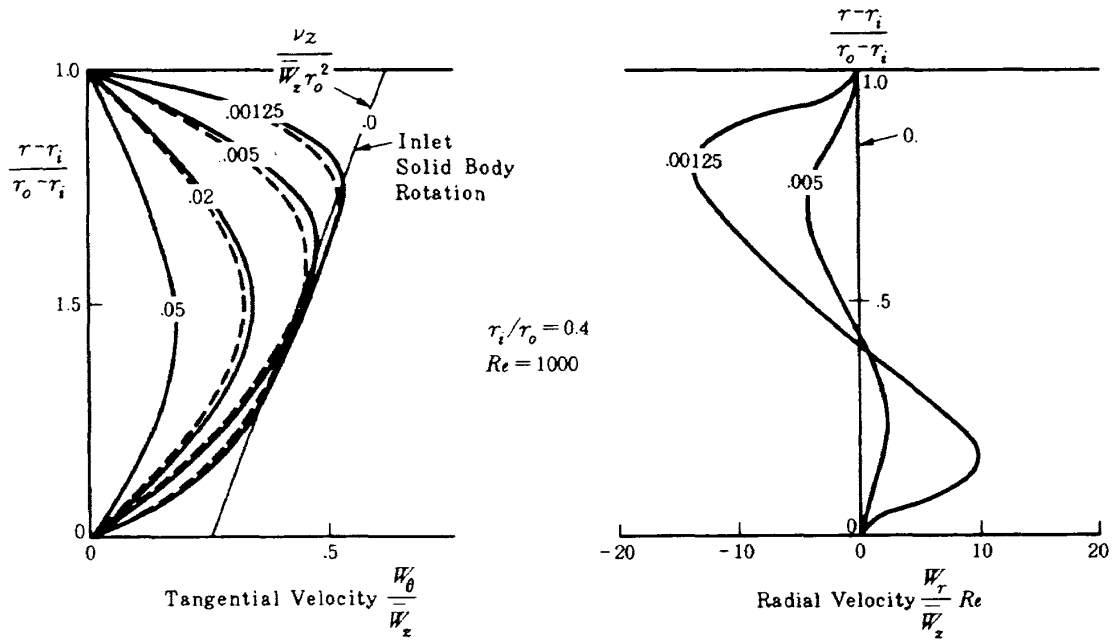

Fig. 4 Laminar Swirling Flow, Comparison of Solutions by Two Methods (---- Scott et. al. (Elliptic N. S. Eq's.) [11], 15 radial × 20 axial grid pts., —— Present (Palabolic N. S. Eq's.), 21 radial grid pts.)

Small difference might have come from the different forms of Navier-Stokes equations employed as well as from numerical errors inherent in both methods; the latter will be examined by refining the mesh. The comparison shows that the present method could be applied to fairly large swirling flows. Fig. 3 shows also the distribution and the rapid decay of raidal velocity component calculated by the present method. On the other hand, the axial velocity profiles and the development were almost same for flows both with and without swirl, which suggests that the equation governing the axial velocity could be handled separately from the equation for the tangential velocity and vice versa; this may justify the separate use of the tangential momentum equation from other momentum equations, to analyze swirling flow problems, as were done by many workers. Since the decay of swirl depends largely on the value of (effective) viscosity,

the decay of turbulent swirling flows would be much greater and pronounced than the laminar flows because of the larger apparent viscosity and of its complex distribution.

Turbulent Flow Without Swirl

Among the annular ducts with r_i/r_o = 0.0625 – 0.562 dealt with by Brighton et al. [12] experimentally, the duct with the smallest ratio of 0.0625 has the most asymmetrical (axial fully developed) velocity profile and is chosen here for the present calculation. Due to the lack of experimental inlet boundary conditions, the calculation has been done by starting from the fully developed laminar flow stage. It would be reasonable to assume "constant" effective viscosity, because of the parabolic velocity profile, to calculate the inlet κ and ϵ. For the initial fully developed laminar flow, the effective viscosity would be equal to the molecular viscosity in principle but it could not be so in order to initiate the turbulent flow calculation.

Fig. 5 was obtained with the inlet effective viscosity of 20 times the molecular viscosity. On the basis of the calculated results, the turbulent eddy (viscosity) would grow from the two near-wall regions very rapidly and interact each other and decrease gradually downstream toward an asymptotic distribution. In Figs. 5 and 6 of the velocity development toward the fully developed turbulent stage calculated with various initial viscosities, one may find an overshooting of the velocity before the fully developed turbulent flow stages (see Ref. 24 for experiment). This final equilibrium velocity profile agrees well with the experimental one except near the inner wall; the equilibrium or universal law of the wall did not give accurate prediction of the velocity profile near the inner wall for small radius ratio such as 0.0625. This was observed also in Brighton's experimental data [12] that significant discrepancy from the universal law of the wall occurs for the inner wall as the radius ratio decreases (i.e., $r_i/r_o < 0.375$). To obtain more accurate prediction, modification has to be needed for the determination of the inner boundary condition. See an example using a different constant for the law of the inner wall [13]. Fig. 6 also shows that very long distance is required to obtain fully developed turbulent flows with any uniform initial viscosities and that the duct length required could not be shortened with an inlet screen with "uniform" mesh in spite of the early rapid development of velocity. Hart et. al. discussed in the Brighton's paper [12] on ineffectiveness of the inlet wall roughness and screen on the entrance length. The final velocity profile and viscosity values at the fully developed stage are not affected by the initial value. The assumption adopted in the present calcula-

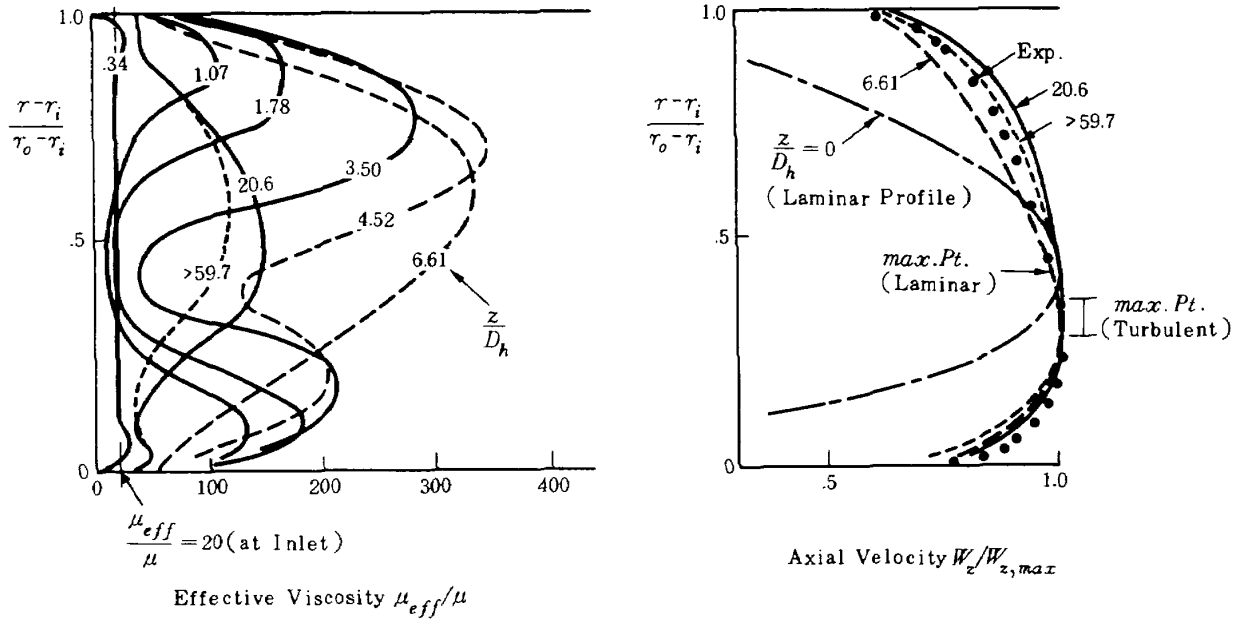

Fig. 5 Turbulent Flow without Swirl, r_i/r_o= 0.0625, Re = 95800, all lines = calculation (15 radial grid pts.), • shows experimental fully developed velocity [12] obtained at z/D_h= 40.5 with roughness element and screen

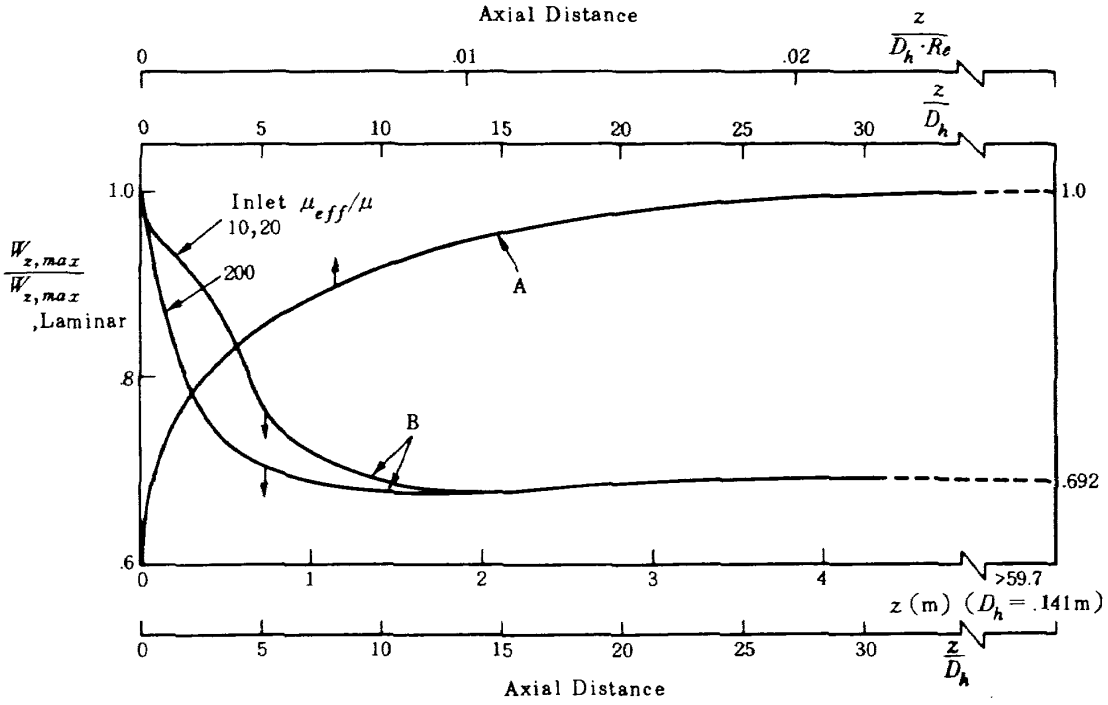

Fig. 6 Variation of Calculated Maxmimum Velocities of Laminar and Turbulent Flows without Swirl Along Annular Duct (r_i/r_o = 0.0625)

A: From Uniform Entrance Flow To Fully Developed Laminar Flow (Re = 1358)

B: From Fully Developed Laminar Flow To Fully Developed Turbulent Flow (Re = 95783)

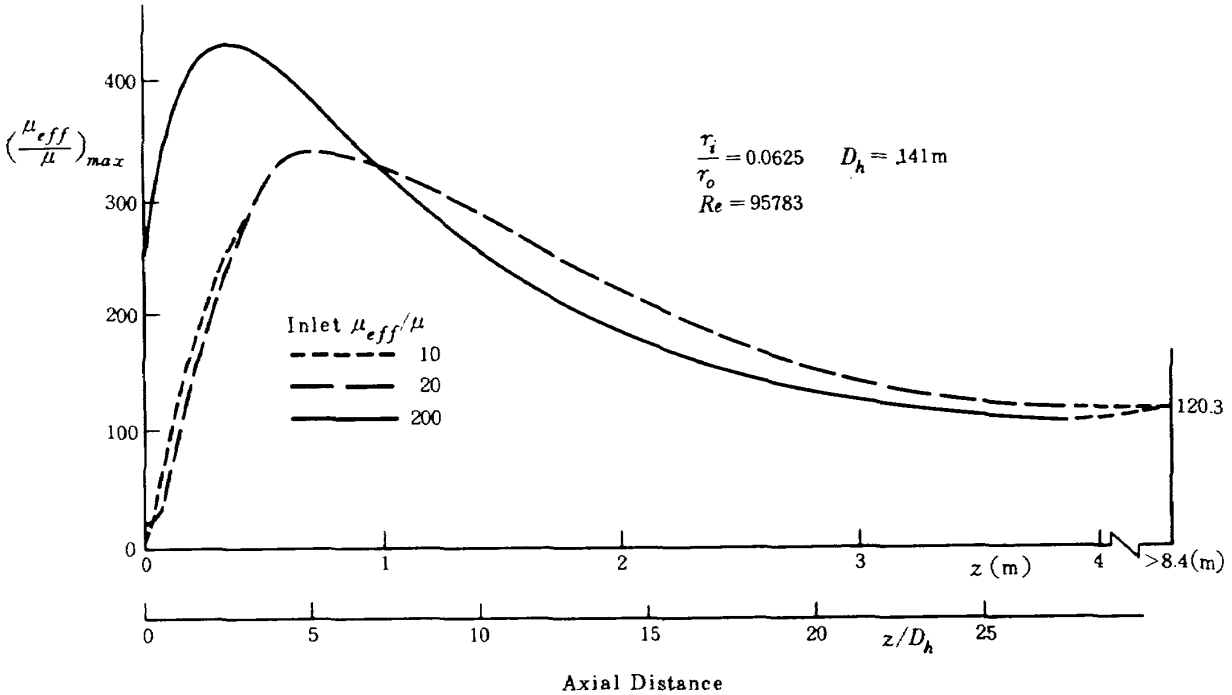

Fig. 7 Variation of Calculated Effective Viscosity Along Annular Duct

tion in order to start turbulent flows as discussed so far, thus, do not have a very serious effect on the large part of the calculation region except near the starting location. Note, however, that an accurate calculation of the initial region is also important in the view of the scale of turbomachinery dimension.

The level of final value of roughly 120 times molecular viscosity as is shown in Fig. 7 seems to be reasonable, based on experimental values reported [e.g. 16, 17], for fully developed turbulent flow in an annulus with about the same Reynolds numbers. Another discovery by Brighton et.al. that the location of the maximum velocity point is nearer the inner wall for turbulent flow than for laminar flow is also well predicted by the present methods as shown in Fig. 5.

Turbulent Flow With Swirl

Recently experimental turbulent eddy viscosities in swirling flow in a stationary annulus with r_i/r_o = 0.4 have been reported by Scott et.al. [18, 19], for flow with initial swirl angle from 0 to 60 degrees. They estimated the axial and tangential effective viscosities from their measured values of velocities and pressures with the aid of simplified momentum equations without shear stress measurement. Fig. 8 shows a complex variation of tangential effective viscosity for a flow with an initial swirl angle of 45 degrees. The corresponding experimental tangential and axial velocity distributions are shown in Fig. 9.

The experimental tangential viscosity at the station 1 was used as the initial viscosity for the present calculation. Fig.10 shows that the axial velocities are excellently predicted but the calculated decay of tangential velocities, however, is much greater than the experimental one, due to the larger calculated viscosities. Other calculations by using different inlet viscosities showed that the initial viscosity had a significant effect on the downstream values of it and therefore on the decay of the swirl as well. Accurate estimation of the viscosity is more important for swirling flows than for non-swirling flows, since the tangential velocity is more affected by the viscosity while the axial velocity is governed strongly by the continuity equation rather than by the value of the viscosity.

In the present study, the equilibrium law of the wall was assumed to govern the velocity near the walls in the tangential as well as the axial direction. The calculated almost symmetrical tangential velocity profiles downstream would have come from the same law of the wall applied to both walls which have dif-

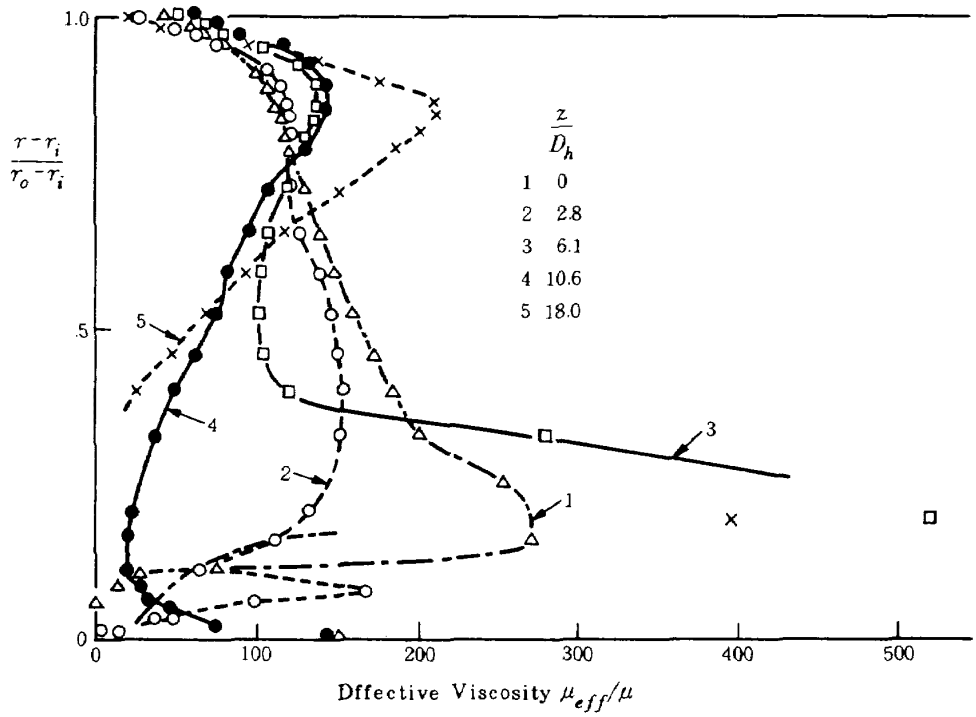

Fig. 8 Distribution of Experimental Tangential Effective Viscosity obtained by Scott et. al. [18], $r_i/r_o = 0.4$, $\phi = 45°$, Re = 130000

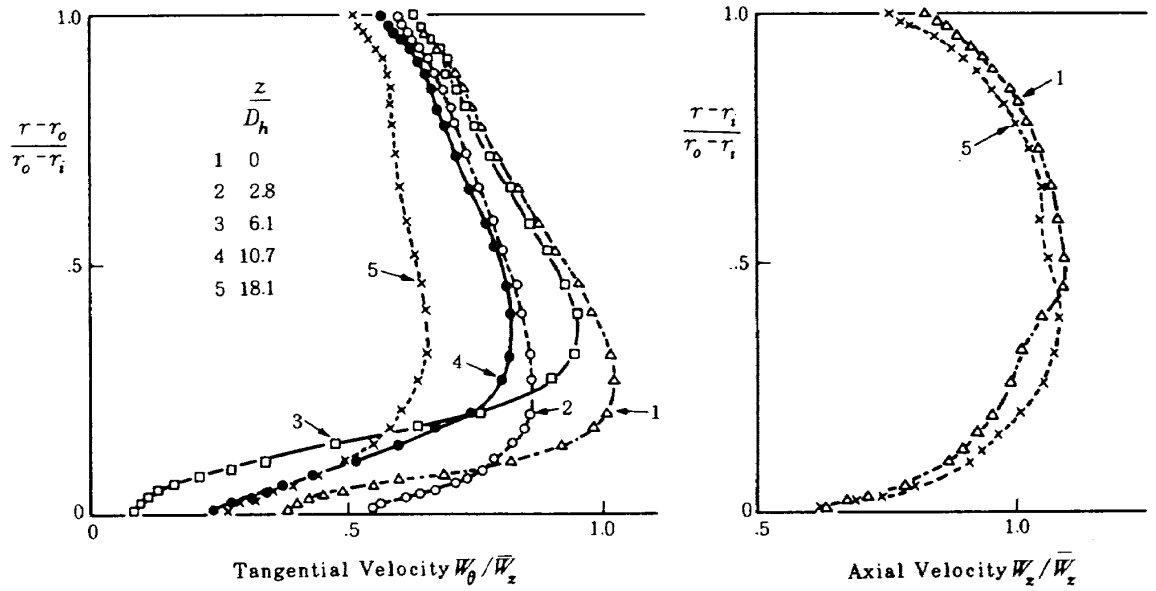

Fig. 9 Experimental Velocity Distribution obtained by Scott et. al. [18], $r_i/r_o = 0.4$, $\phi = 45°$, Re = 130000

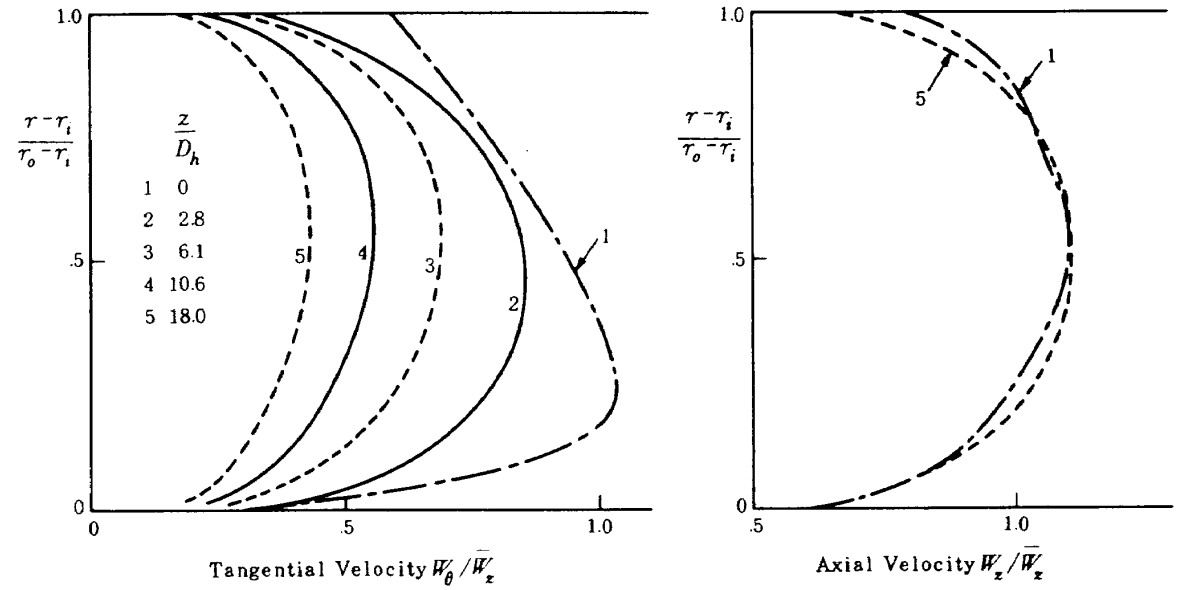

Fig. 10 Calculated Results of Turbulent Swirling Flow, $\frac{r_i}{r_o} = 0.4$, $\phi = 45°$, Re = 130000, 21 radial grid pts.

ferent curvatures in the circumferential direction and two oppositely distributed radial pressure gradients due to the centrifugal force. As seen in Fig. 10, a much larger discrepancy from the experimental tangential velocity profiles can be seen especially near the outer wall as compared to those near the inner wall. Following comments would be useful to understand this situation and to improve the method: Bradshaw [14] states that, for convex curvature, the centrifugal force tends to stabilize the turbulence, but, for a concave surface, tends to destabilize it. He correlates the effect on the Prandtl's mixing length using Richardson number and Sharma et al. used the above correlation for two types of swirling flows [7, 20] where Richardson number is always negative or zero (turbulence promoted). McDonald [21] also reports the similar effect in terms of streamwise pressure gradient on the law of the wall although effect

of the pressure gradient normal to the wall has not been clear. The "equilibrium" state might be basically impossible in swirling flows until the swirl decays completely.

Similarly to what was seen before in non-swirling flow, the viscosity increases first and then decreases in the present case of swirling flow, too. No other experiment nor calculations have been reported on this kind of behaviour of effective viscosity at the early state of flow (i.e., not fully developed stage), so further discussion might be of little value. Fig. 11 shows the variation of velocities and effective viscosity along the annular duct. Although the reliability of the experimental effective viscosity of a swirling flow referred here is in question because of indirect measurement of shear stresses and turbulent intensity, the values presently calculated are considered to be within the range of physical possible values.

Presently calculated distributions of effective viscosity had single central peak at fully developed stage opposed to the experimental double peaks and then study is now progressing on adjusting the empirical constants used in the turbulence model with proper modification of boundary conditions and an experimental work of swirling flows is also being conducted at NAL.

FURTHER APPLICATIONS AND EXTENSIONS

The present 'viscous' code was applied to also some rotating annular passages to see similar velocity profiles of fluid as often seen at the exits of rotating passages or rotors of turbomachinery. In this example, the flow passes through a rotating passage first where the inner and outer walls rotates with a same angular velocity (as solid body) and then it enters a stationary passage as shown in Fig. 12. The flow which has initially a uniform axial velocity only will have tangential velocity by the fluid viscous forces acting between the fluid and the walls. This is shown by some dash lines in the same figure. The velocity profile of the flow would have finally that of solid body rotation if the rotating duct is long enough. When the flow enter the stationary duct at $z^*=0.048$, the fluid at the walls should have the corresponding wall velocities. Calculation with this sudden discontinuity condition was accomplished without any problems and shown by solid lines. From the calculated results just after the exit of the rotating passage ($z^*=0.00125$) one may recognize a similar velocity profile to experimental rotor exit velocity which are often found in turbine and compressor tests but have never been well predicted by any inviscid calcu-

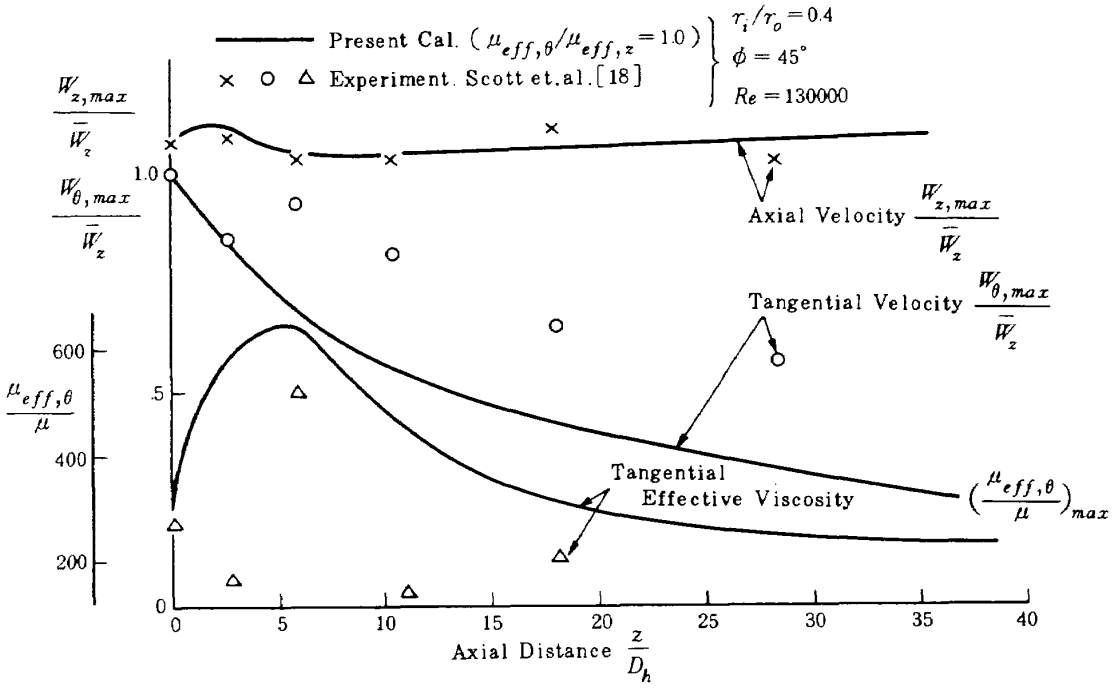

Fig. 11 Variation of Calculated Maximum Velocities and Effective Viscosity along an Annular Duct (Turbulent Swirling Flow)

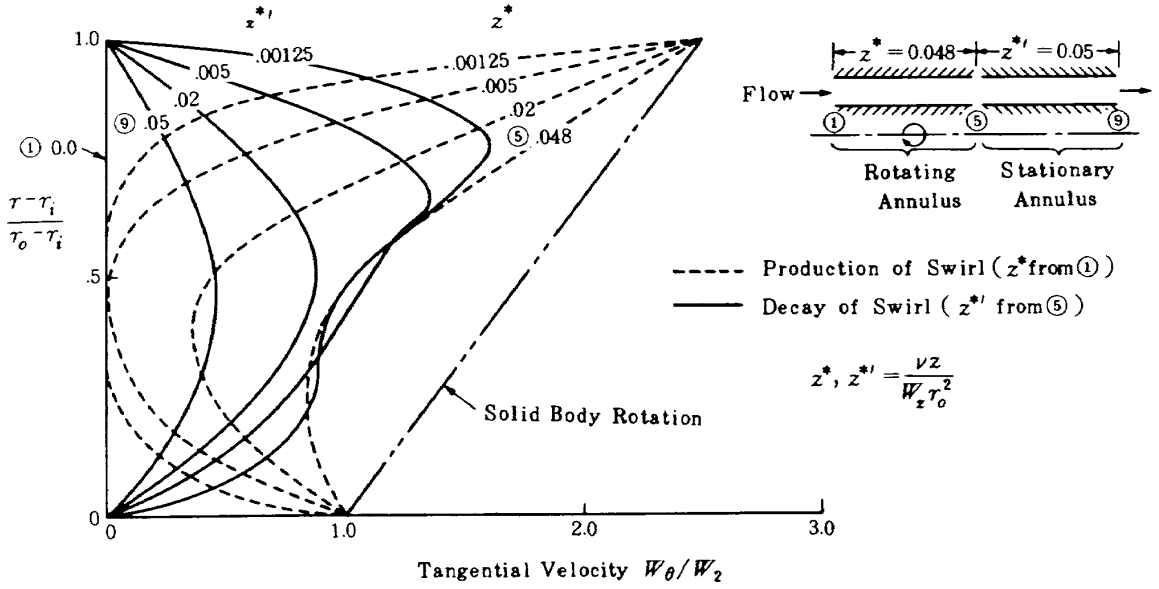

Fig. 12 Production of Swirl in Rotating Annulus and Decay of Swirl in Stationary Annulus, $r_i/r_o = 0.4$, Re = 1000, Laminar Flow

lation methods used for turbomachinery design and performance prediction such as [1].

An extention of the present program was done [28] by replacing the boundary condition (law of the wall) used at the walls with that of so-called low Reynolds number turbulence model. This modification enabled no-slip condition to be used at the walls much more easily but needed more computer time and storage. A calculated result is shown in Fig. 13 which seems to show much more realistic behavior of effective viscosity in comparison with experimental data.

The program has been originally written in an orthogonal coordinates as shown Fig. 14, [5]. Calculation of curved duct may be interesting. The program can be extended to calculate cascade flows as shown in Fig. 15 which meshes were generated by applying the transformation program of Thompson et. al. [25] to a NAL air-cooled turbine nozzle [26] In this case, Navier-Stokes equations of elliptic type or time dependent parabolic type (elliptic in space) should be more useful to analize the flow because the important occurrence of flow separation from the blade surfaces and/or trailing edge could be handled by these equations. This could be done practically without any problem if the flow assumed to be 2 dimensional or laminar (e.g. see Fig. 16, [25]). The types of computer code presently available could be summarized as shown in Table 3.

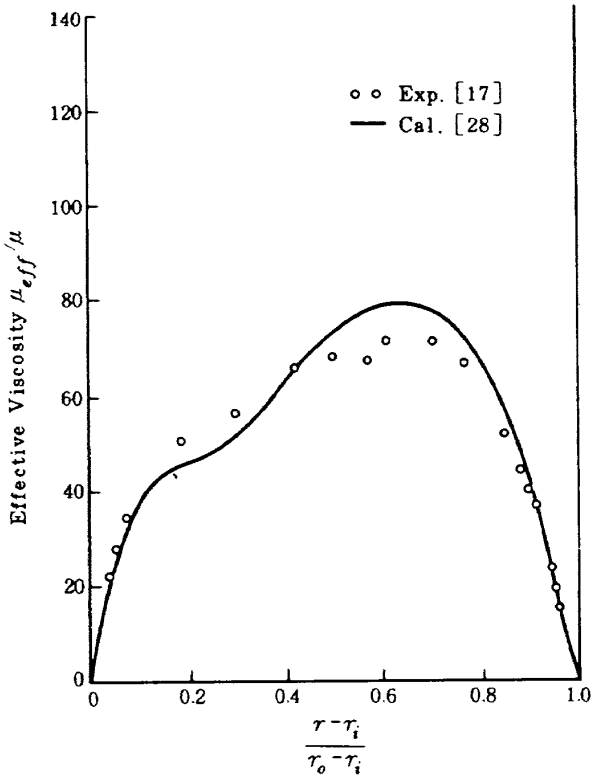

Fig. 13 Calculated Effective Visconsity with Low Reynolds Number Turbulence Model, Turbulent Flow without Swirl, $r_i/r_o = 0.178$, Re = 519000

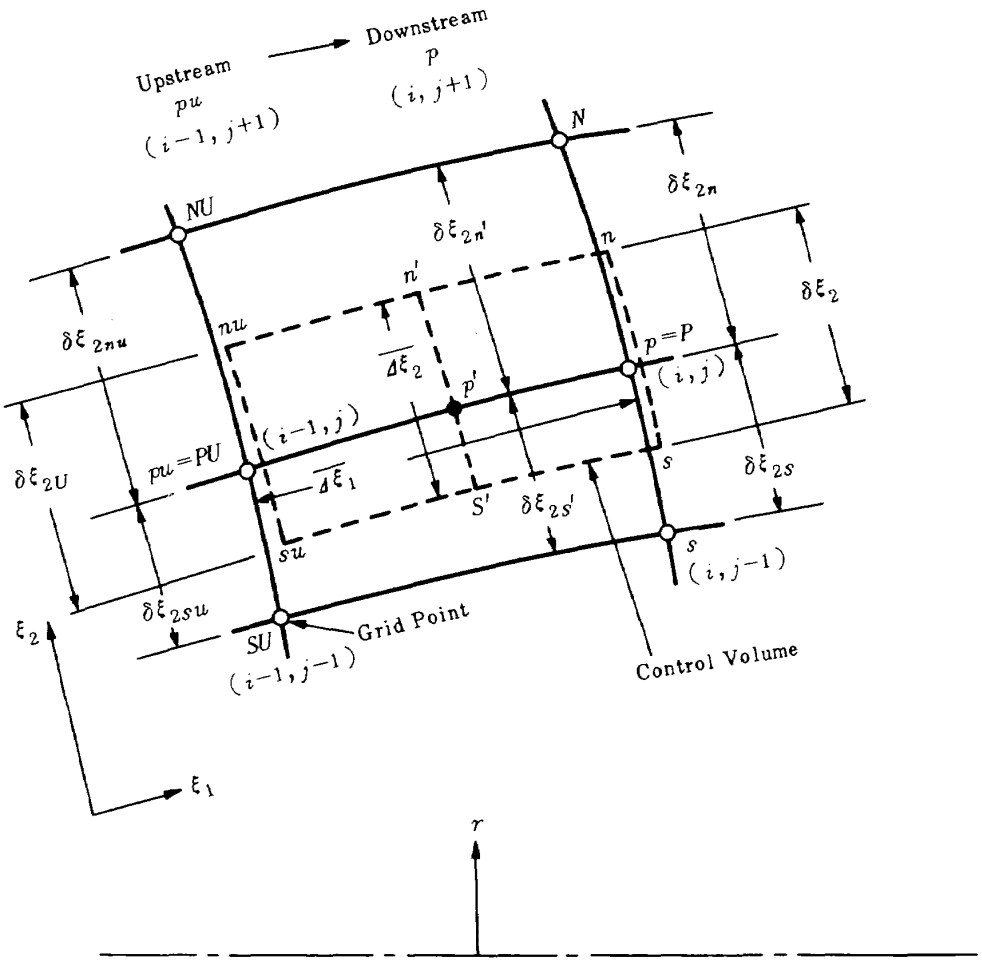

Fig. 14 Finite Difference scheme for orthgonal Coordinates

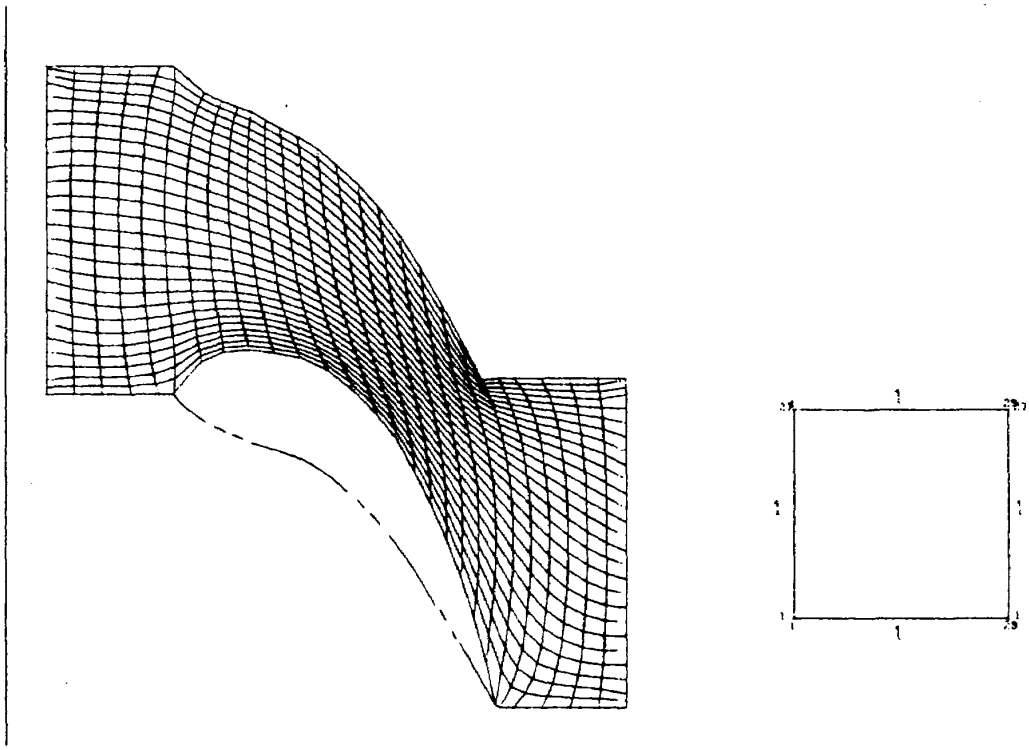

Fig. 15 Mesh Generation for Computation, NAL Air-Cooled Turbine Nozzel [26], Transformation Case 1

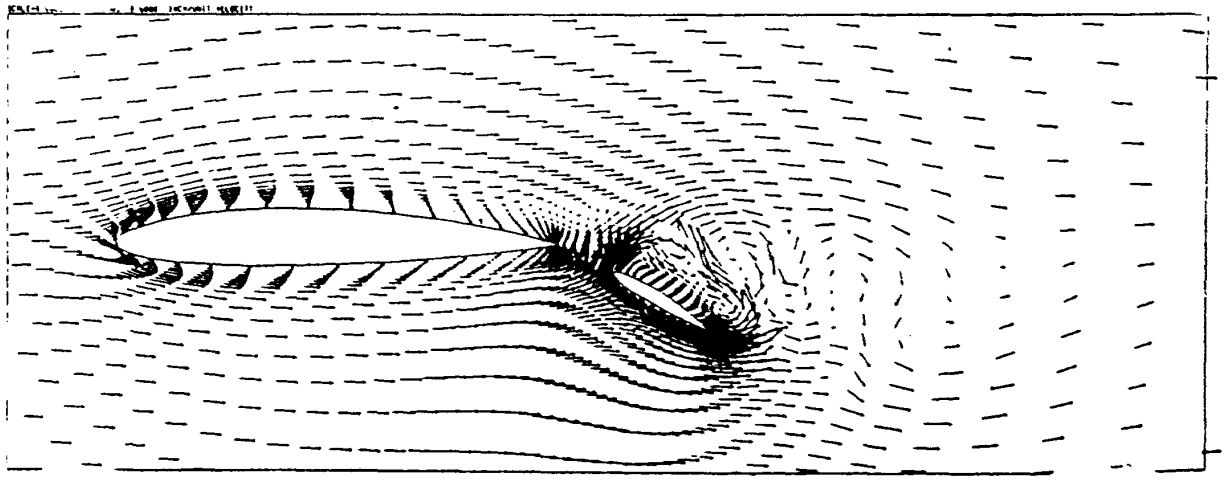

Fig. 16 Viscous Flow Solution around Aerofoil
Re = 1000, t = 3.02, [25]

Table 3 Rough Survey of Soluvable Navier-Stokes Equation Types**

TYPE		2-D.	3-D.
Steady Parabolic	a.	$\frac{\partial^2}{\partial Z^2} = 0$ (streamwise = z)	$\frac{\partial^2}{\partial Z^2} = 0$
	b.	High Re	low, mid Re
	c.	1 min. (laminar), CDC6600 5 min. (2-Eq's T. mode), XEROX S.-9	3 min. (laminar), IBM7094
	d.	impossible	impossible
Unsteady Parabolic*	a.	Thin-layer Approx.	Thin-layer Approx.
	b.	High Re	High Re
	c.	16 min. (laminar, 71 x 27), CDC7600	2-3 hrs. (laminar, 30 x 30), CDC7600
	d.	possible	possible
Elliptic ($\frac{\partial^2}{\partial Z^2} \neq 0$)	a.	Steady	Unsteady
	b.	High Re	Low Re
	c.	1.5 min. (laminar, 13 x 13) CDC6600 3 hrs. (laminar, 81 x 81), CDC6600	3-15 hrs. (laminar, 11 x 11 x 21), UNIVAC1108
	d.	possible	possible

	a.	b.	c.	d.
Partially Parabolic (3-D)	$\frac{\partial^2}{\partial Z^2} = 0$, $\neq 0$ for p	Low Re,	14 min. (70 x 18 x 17), CDC6600,	?

Notes: a. Assumptions
b. Re No. soluvable (eg. mid Re = 1000 - 2000)
c. CPU time (flow, mesh), Computer
d. Streamwise Separation
* Parabolic relative to time but elliptic relative to space
** Survey in Sept. 1978

CONCLUSIONS

A systematic study of laminar and turbulent swirling flows in annuli analized in the present calculations showed reasonable and possible patterns and shows that the present approach is promissing for the prediction. In the present calculation procedures, the determination of the wall boundary conditions were most important and the method by the equilibrium or universal law of the wall was not so appropriate as expected to predict the axial velocity near the inner wall even for non-swirling flow in annuli with small inner/outer radius ratio and to predict the tangential velocity especially near the outer wall for swirling flow. The problem of turbulent swirling flow in stationary annuli is still difficult to analize because of the lack of reliable experimental data on turbulent momentum transport coefficients in this skewed flow, and therefore it needs further experimental study as well as theoretical approaches.

ACKNOWLEDGEMENTS

This work was supported by the National Research Council of Canada under Grant No. A1676. One of the authors (A.Y.) appreciates also the cooperation of the Canada Council for the 2 year scholarship (1977-1978).

REFERENCES

1. Davis, W. R., and Millar, D. A. J., A Comparison of the Matrix and Streamline Curvature Methods of Axial Compressor Analysis, from Users Point of View, *Journal of Engineering for Power, Trans. of ASME*, Vol. 97, p. 549, 1975
2. Launder, B. E., and Spalding, D. B., The Numerical Computation of Turbulent Flows, *Computer Methods in Applied Mechanics and Engineering*, Vol. 3, p. 269, 1974
3. Launder, B. E., and Spalding, D. B., Turbulence Models and Their Application to the Prediction of Internal Flows, *Heat and Fluid Flow*, Vol. 2, p. 43, 1972
4. Bobkov, V. P., Ibragimov, M. Kh., and Sabelev, G. I., Correlation of Experimental Data on the Pulsation Velocity Intensity for Turbulent Fluid Flow in Channels of Different Form, *Fluid Dynamics*, Vol. 3, p. 111, 1968
5. Yamamoto, A., A Method for Calculating Laminar and Turbulent Swirling Flow in Cylindrical Annuli, *M. Eng. Thesis (1978)*, Carleton University
6. Lui, J., and Shah, V. L., Flow of a Bingham Fluid in the Entrance Region of Annular Tubes, *Advances in Computer Method for Partial Differential Equations* (Edited by Vichnevetsky, R.), Publ. AICA, p. 230, 1975
7. Sharma, B. I., Launder, B. E. and Scott, C. J., Computation of Annular, Turbulent Flow with Rotating Core Tube, *Journal of Fluid Engineering, Trans. of ASME*, Vol. 98, p. 753, 1976
8. Rose, M. E., On the Integration of Non-Linear Parabolic Equations by Implicit Difference Methods, *Quarterly Applied Mathematics*, Vol. 14, p. 237, 1956
9. Fredicton, A. G., and Bird, R. B., Non-Newtonian Flow in Annuli, *Industrial Engineering Chemistry*, Vol. 3, No. 4, p. 383, 1958
10. Patankar, S. V., and Spalding, D. B., *Heat and Mass Transfer in Boundary Layers*, 2nd Edition, Intertext Books, London, 1970
11. Scott, C. J. and Bartelt, K. W., Decaying Annular Swirl Flow with Inlet Solid Body Rotation, *Journal of Fluid Engineering*, Vol. 98, p. 33, 1976
12. Brighton, J. A., and Jones, J. B., Fully Developed Turbulent Flow in Annuli, *Journal of Basic Engineering*, Vol. 86, p. 835, 1964
13. Hanjalic, K., and Launder, B. E., A Reynods Stress Model of Turbulence and Its Application to Thin Shear Layer, *Journal of Fluid Mechanics*, Vol. 52, p. 609, 1972
14. Bradshaw, P., Turbulent Boundry Layer, *The Aeronautical Journal of the Royal Aeronautical Society*, Vol. 72, p. 452 (Discussion with Ntim on p. 459), 1968
15. McDonald, H., Practical Calculations of Transitional Boundary Layers, *International Journal of Heat and Mass Transfer*, Vol. 16, p. 1729 (See discussion on the transitional location on p. 1737), 1973
16. Ramm, H., Theoretisches Modell zue Beschreibung des Impuls und Energietransports in Turbulenter Kanalströmung, *Doctor Dissertation*, Vom Fachbereich Verfahrenstechnik (FB 10) der Technischen Universitat Berlin, 1974
17. Quarmby, A., and Anand, R. K., Turbulent Heat

Transfer in the Thermal Entrance Region of Concentric Annuli with Uniform Wall Heat Flux, *International Journal of Heat and Mass Transfer*, Vol. 13, p. 395, 1970

18. Scott, C. J., and Rask, D. R., Experimental Turbulent Viscosities for Swirling Flow in a Stationary Annulus, *University of Minnesota, Dept. of Mechanical Engineering, HTL* TR No. 94, 1971
19. Scott, C. J., and Rask, D. R., Turbulent Viscosity for Swirling Flow in a Stationary Annulus, *Journal of Fluid Engineering, Trans. of ASME*, Vol. 95, p. 557, 1973
20. Sharma, B. E., Computation of Flow Past a Rotating Cylinder with an Energy-Dissipation Model of Turbulence, *AIAA Journal*, Vol. 15, No. 2, p. 271, 1977
21. McDonald, H., The Effect of Pressure Gradient on the Law of the Wall in Turbulent Flow, *Journal of Fluid Mechanics*, Vol. 35, p. 311, 1969
22. Bissonnette, L. R., and Mellor, G. L., Experiments on the Behaviour of an Axisymmetric Turbulent Boundary Layer with a Sudden Circumferential Strain, *Journal of Fluid Mechanics*, Vol. 63, p. 369, 1974
23. Abdel-Gayed, R. G., and Bradley, D., Derivation of Turbulent Transport Coefficients from Turbulent Parameters in Isotropic Turbulence, *Journal of Fluid Engineering, Trans. of ASME*, Vol. 99, p. 732, 1977
24. Bradshaw, P., Dean, R. B., and McEligot, D. M., Calculation of Interacting Turbulent Shear Layers: Duct Flow, *Journal of Fluids Engineering, Trans. of ASME*, Vol. 95, p. 214, 1973
25. Thompson, J. F., Thames, F. C., and Mastin, C. W., Boundary-Fitted Curvilinear Coordinate Systems for Solution of Partial Differential Equations on Fields Containing Any Number of Arbitrary Two-Dimensional Bodies, *NASA CR-2729*, 1977
26. Yamamoto, A., Takahara, K., Nouse, H., Inoue, S., Usui, H., and Mimura, F., Aerodynamic Investigation of an Air-Cooled Axial-Flow Trubine, Part I Turbine Design and Overall Stage Performance without Supply of Cooling-Air, *NAL TR-321 (NASA TT F-16083)*, 1973
27. Yamamoto, A. and Millar, D. A. J., A Calculation of Laminar and Turbulent Swirling Flows in Cylindrical Annuli, Symposium on Flow in Primary, Non-Rotating Passages in Turbomachines, *ASME Winter Annual Meeting (New York)*, 1979
28. Yamamoto, A., Shibuya, Y. and Nouse, H., Theoretical Prediction of Turbulent Momentum Transport Quantities in Annular Ducts, to be published, See also Brief Notes of B. Engng. Thesis, p. 87 (Shibuya), *Faculty of Mech. Engng.*, University of Nippon, 1979

既　刊　報　告

TR-630	液体の入った球型シェルの振動解析 －付加質量系数を用いた解析 Vibration Analysis of Spherical Shells Partially Filled With a Liguid	1980年10月	小松　敬治
TR-631	低速で高揚力を得るための多翼素翼型の設計 A Design of Multi-Element Aerofoils for High Lift	1980年10月	重見
TR-632	二次元振動翼まわり非粘性遷音速流の差分法による数値計算 Finite Difference Calculations of Inviscid Transonic Flows Over Oscillating Airfoils	1980年10月	石黒登美子
TR-633	スキャン型地球センサの解析評価 Analysis and Evaluation of Conical Scanning Earth Sensors	1980年10月	木田　隆，[illegible]　嘉彰 鈴木　崇弘，若[illegible]　清央
TR-634	高膨張ロケットノズル内の流れの計算について An Investigation of the Numerical Methods for the High-Expansion Rocket Nozzle Flow Calculation	1980年10月	中橋　和博，毛　明夫 宮島　博
TR-635	高性能推進薬の研究 －酸素・リチウム・水素プロペラント－ High Performance Propelant Study-Oxygen Lithium Hydrogen Tripropellant	1980年10月	毛呂　明夫，鈴木　和雄
TR-636	遷音速風胴模型の姿勢自動設定 Autmatic Attitude Setting of a Wind Tunnel Model in a Transonic Wind Tunnel	1980年10月	波木井[illegible]潔，小池　陽
TR-637	推力大きさ制御型固体ロケット・モータの燃焼実験 （第1報　300φ端面燃焼方式） Firing Tests of Thrust Controllable Solid Rocket Motors Part 1：300-mm-Diameter and Burning Grain Moter：	1980年11月	五代　富文，清水　盛生 伊藤　克弥，種村　利春 藤原　勉，日下　和夫 木皿　且人，伊藤　政裕 髙橋　守，泉川　宗男
TR-638	ロケット地上燃焼実験時のロードセル最大荷重と推力立上り特性の推定 Prodiction of the Maximum Force Acting of the Loodcell and Thrust Transient Durin Rocket Motor Firing Tests	1980年11月	工藤　賢司，村上　淳郎 小室　智幸，石井　進一 梶原　堅一
TR-639	吹出式風洞用高圧貯気槽設備の定温装置の特性測定と第3高圧貯気槽の増設 Characteristics of a Simple Capacity Heat Exchanger in High Pressure Storage Vessels for NAL Blow Down Wind Tunnels and the Construction of a 3rd High Pressure Storage Vessel	1980年11月	鈴木　誠三，萱場　重男 野口　正芳，小松　行夫 鈴木　正光，萩原　[illegible]

TECHNICAL REPORT OF NATIONAL AEROSPACE LABORATORY
TR-640T

航空宇宙技術研究所報告640T号（欧文）

昭和55　11月発行

発行所　航空宇宙技術研究所
東京都調布市深大寺町1880
電話武蔵野三鷹(0422)47-5911(大代表)〒182

印刷所　株式会社　三興印刷
東京都新宿区信濃町12　三河ビル

Published by
NATIONAL AEROSPACE LABORATORY
,880 Jindaiji, Chōfu, Tokvo
JAPAN